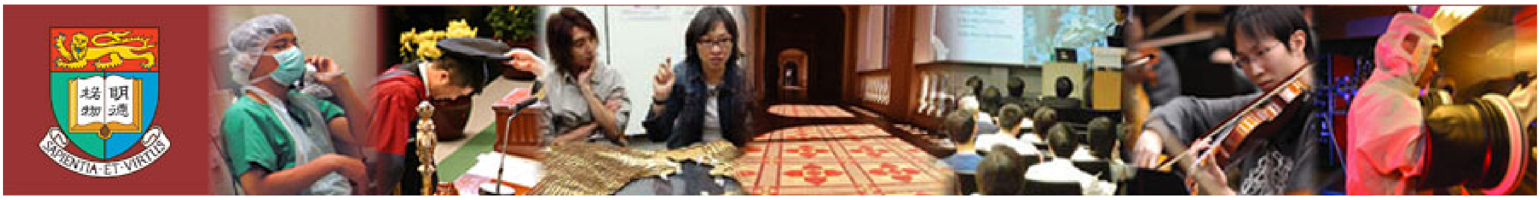

Title	Enhanced structural and magnetic ordering of FePt/Mn-oxide bilayers by ion-beam bombardment and annealing
Author(s)	Sun, AC; Hsu, HF; Wu, HJ; Hsu, JH; Pong, PWT; Suzuki, T; Lin, KW
Citation	The 2010 Asia-Pacific Data Storage Conference (APDSC'10), Hualien, Taiwan, 27-29 October 2010. In IEEE Transactions On Magnetics, 2011, v. 47 n. 3, p. 501-504
Issued Date	2011
URL	http://hdl.handle.net/10722/126046
Rights	IEEE Transactions on Magnetics. Copyright © IEEE.

Enhanced Structural and Magnetic Ordering of FePt/Mn-Oxide Bilayers by Ion-Beam Bombardment and Annealing

An-Cheng Sun[1], H.-F. Hsu[2], H.-J. Wu[2], J.-H. Hsu[3], P. W. T. Pong[4], T. Suzuki[5], *Fellow, IEEE*, and K.-W. Lin[2]

[1]Department of Chemical Engineering & Materials Science, Yuan Ze University, Chung-Li 32003, Taiwan
[2]Department of Materials Science and Engineering, National Chung Hsing University, Taichung 402, Taiwan
[3]Department of Physics, National Taiwan University, Taipei 106, Taiwan
[4]Department of Electrical and Electronic Engineering, The University of Hong Kong, Hong Kong
[5]MINT Center, University of Alabama, Tuscaloosa, AL 35487 USA

Structural and magnetic properties of FePt thin films were affected strongly by capped MnO_x layers prepared by ion-beam bombardment and post-annealing. As-deposited $FePt/MnO_x$ bilayer exhibited a magnetically soft fcc phase, and it turned to an ordered fct FePt phase with large coercivity (∼8 kOe) after annealing at 550°C. Increasing the $\%O_2/Ar$ in capped MnO_x layer during deposition resulted in smaller ordered FePt grains separated by grain boundaries of MnO_x. We found that the superlattice (001) peak is broadened considerably with larger amount of MnO_x incorporated into FePt, likely due to the hindered formation of hard phase. Our results indicate that $FePt/MnO_x$ films deposited with lower $\%O_2/Ar$, the oxygen atoms may occupy the interstitial positions in the FePt lattice to induce a local strain thus enhancing the FePt ordering. Further increased $\%O_2/Ar$ in capped MnO_x layer, the excess oxygen atoms act a diffusion barrier effectively to inhibit the FePt grain growth and ordering.

***Index Terms*—FePt, ion-beam bombardment, magnetic films, phase transformation.**

I. Introduction

ORDERED FePt films have been considered as one of the most promising candidates for future ultra-high density magnetic recording media [1]–[8] due to their large magnetocrystalline anisotropy ($K_u \sim 7 \times 10^7$ ergs/cc) that can enable the minimal magnetic stable grain size of FePt to be smaller than 5 nm [9]. In order to fulfill the requirements of magnetic recording application, to optimize the microstructures and magnetic properties, decoupled and ordered FePt grains is necessary [10]. Different oxides such as SiO_2 [11], TiO_2 [7], and Ta_2O_5 [12] are chosen to add into FePt films to control the grain size and exchanged coupling effectively. Our previous works [13]–[15] also showed that using ion-beam bombardment during film deposition can effectively modify the film microstructure as well as magnetic properties, and post-deposition annealing can further modify the nanomagnetism of the film. FePt grain separation can be achieved by incorporating different amounts of oxygen using an ion-beam deposition technique [13]. In this paper, Mn-oxide capping layers with different oxygen contents prepared by an ion-beam bombardment technique [16] and annealing were used to investigate the effect of oxygen contents on film microstructures, ordering parameters, and magnetic properties. It has been found that FePt grains were well separated by grain boundaries of Mn-oxide in annealed FePt/MnO_x bilayers, while the film as a whole maintained a moderate perpendicular coercivity, that show potential for magnetic recording applications.

Manuscript received September 16, 2010; accepted December 01, 2010. Date of current version March 02, 2011. Corresponding author: K.-W. Lin (e-mail: kwlin@dragon.nchu.edu.tw).

Color versions of one or more of the figures in this paper are available online at http://ieeexplore.ieee.org.

Digital Object Identifier 10.1109/TMAG.2010.2099111

II. Experimental Methods

The co-sputtering FePt films (10 nm) on thermal oxide SiO_2 substrates were prepared by an UHV magnetron sputtering system [11] while the capping Mn-oxide layers (10 nm) were deposited by using the dual ion-beam deposition technique [13], [17]. A Kaufman source (800 V, 7.5 mA) was used to focus an argon ion beam onto a commercial Mn target surface while the End-Hall source ($V_{EH} = 100$ V) was used to in-situ bombard and clean the substrates during the Mn-oxide deposition with a mixture of O_2/Ar gas. The oxygen content of the O_2/Ar gas was varied from 8% to 41% O_2/Ar. The samples were post-annealed at 550°C for 10 min in an UHV chamber. No external magnetic field was applied during deposition. The crystal structures of FePt/MnO_x bilayers were characterized by grazing angle (1^o) X-ray diffraction (XRD) using a Bruker D8 SSS diffractometer (Cu $K\alpha$ radiation). A JEOL (JEM-2010) transmission electron microscope (TEM) operating at 200 kV was used for the microstructural analysis. Magnetic properties were performed with a commercial vibrating sample magnetometer (VSM) with maximum magnetic field of 20 kOe at room temperature (RT). Surface morphology and magnetic domain structures were characterized by using a Seiko SPI 3800 N atomic force microscopy/magnetic force microscopy (AFM/MFM).

III. Results and Discussion

A. *Temperature Dependence on Formation of Ordered fct FePt Phase*

The structures of as-deposited at RT and post-annealed FePt/MnO_x (8% O_2/Ar) bilayer films characterized by XRD are shown in Fig. 1. The annealing conditions are 350 to 550°C for 10 min. The as-deposited FePt/MnO_x bilayer film exhibited fcc FePt phase, as indexed by the (111) and (200) reflections of FePt structures in Fig. 1, that resulted from intermixing of Fe and Pt atoms during deposition. The same (111) reflections of

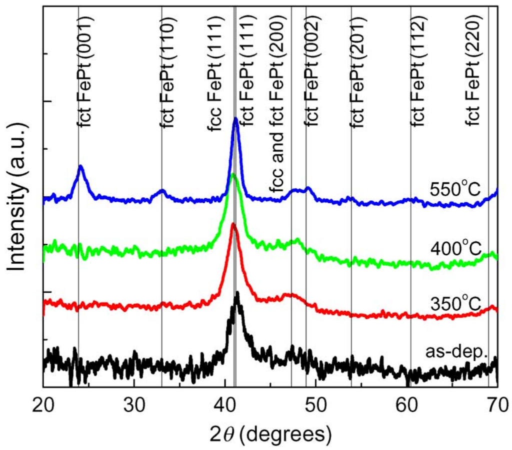

Fig. 1. XRD patterns of as-deposited and post-annealed FePt/MnO_x (8% O_2/Ar) bilayer films. The annealing conditions are 350 to 550°C for 10 min.

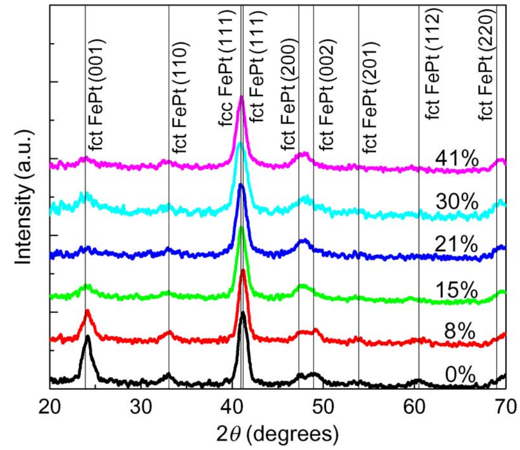

Fig. 2. XRD patterns of 550°C annealed FePt/MnO_x bilayer films. The MnO_x fraction was changed from 0% to 41% O_2/Ar.

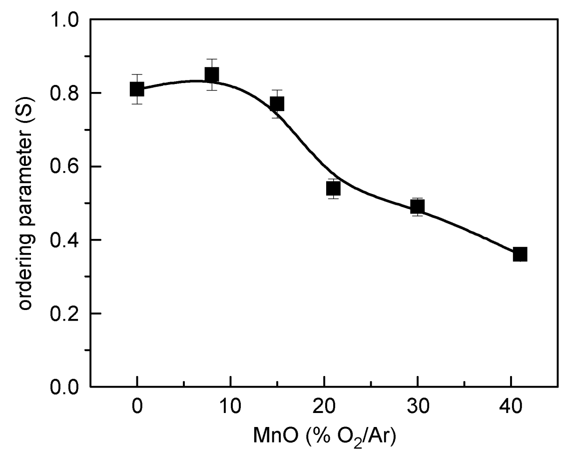

Fig. 3. The dependence of $L1_0$ ordering parameters various MnO_x % O_2/Ar.

disordered fct FePt (111) structures were observed at $2\theta \sim 41°$ for films annealed at 350 and 400°C, respectively. However, further increasing the annealing temperatures from 400 to 550°C resulted in structural phase transformation from fcc FePt to fct FePt ($a \sim 3.85$ Å, $c \sim 3.73$ Å), indicating the onset of structural phase transformation occurs at greater than 400°C. This is evidenced by the increased intensities of ordered FePt phases such as fct(001), fct(110), fct(002) reflections in Fig. 1 and confirmed by the peak shift of (111) reflections from fcc ($2\theta \sim 41°$) to fct ($2\theta \sim 41.5°$). The hysteresis loops of 400 and 550°C post-annealed FePt/MnO_x (8% O_2/Ar) bilayer films were also determined (data no show) where the applied field was perpendicular to the film plane during measurement. The magnetic properties were consistent with the phase structure change. The 400°C annealed FePt/MnO_x bilayer film were magnetically soft ($H_c \sim 200$ Oe), attributed to the disordered fcc FePt phases [13]. However, H_c was significantly increased to about 8 kOe as annealing temperature increased to 550°C, suggesting an increasing amount of harder fct FePt phases in FePt/MnO_x bilayer films.

B. *Effects of Oxygen Content on Microstructures, Ordering Parameters, and Magnetic Properties of Ordered fct FePt Phase*

In order to understand the influence of MnO_x contents on structures, FePt/MnO_x bilayer films with various O_2/Ar fractions were annealed at 550°C for 10 min and the results were presented in Fig. 2. The annealed pure FePt films (0% O_2/Ar) exhibits ordered $L1_0$ FePt phases, as indexed by the fct(001), fct(110), fct(111), fct(002), etc., reflections shown in Fig. 2. As addition of MnO_x from 8% to 41% O_2/Ar, similar FePt structures were found during deposition, however, the variations in the diffraction peak intensity of, e.g., the (001), (110), and (002) reflections, were observed that depended on the amounts of MnO_x incorporated into the FePt films. The evidences are the decreased intensities of ordered FePt phases such as (001), (110), (002) reflections and the peak shift of (111) reflections from fct ($2\theta \sim 41.5°$) to fcc ($2\theta \sim 41°$) in Fig. 2. This implies that the top MnO_x layer diffused effectively into the bottom FePt layer during post-annealing and affected the peak intensity in XRD patterns.

The order parameters (S) [18] of these annealed FePt/MnO_x bilayer films with various oxide contents were shown in Fig. 3. It was found that the pure FePt layer exhibited an order parameter of $S \sim 0.81$ whereas a slightly increase to 0.85 was observed in annealed FePt/MnO_x bilayer film when made with 8% O_2/Ar. However, reduction of S was found in samples with further addition of MnO% O_2/Ar. Therefore, few amount doped MnO_x is helpful for phase transformation from fcc FePt into fct FePt. When the amount of MnO_x is over a critical value, the excess oxygen atoms may turn to the diffusion barrier for FePt grain ordering.

From the structure characterization (Fig. 2) we already knew the phase structures were affected with different fractions of MnO% O_2/Ar. Thus, it is important to understand the morphology and distribution of MnO_x in the ordered FePt phases. Therefore, TEM was carried out here on the annealed FePt/MnO_x bilayer films with 8% and 41% of O_2/Ar, and the results were shown in Fig. 4(a) and (b), respectively. In Fig. 4(a), nonuniform FePt grains and distribution were found in annealed 8% O_2/Ar FePt/MnO_x bilayer film. The grain sizes ranged from 5 to 10 nm. However, 2 or 3 grains connected

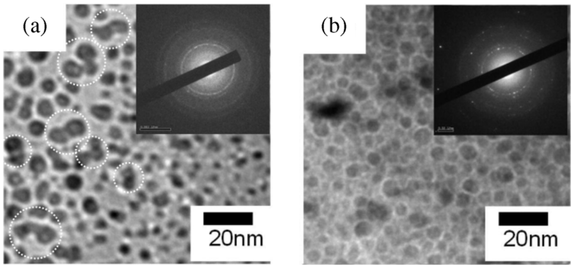

Fig. 4. Plane-view TEM micrographs of (a) the annealed FePt/MnO_x (8% O_2/Ar) bilayer and (b) the annealed FePt/MnO_x (41% O_2/Ar) bilayer. The corresponding electron diffraction patterns are shown in the insets of each figure. The annealing conditions are 550°C for 10 min.

well and come out a larger FePt grain with size of 20 nm, which were indexed by circles in Fig. 4(a). The large grain size distribution is attributed to the coalescence of FePt grains during post-annealing [14]. The electron diffraction patterns of annealed 8% O_2/Ar FePt/MnO_x bilayer film [the inset of Fig. 4(a)] exhibited $L1_0$ FePt phases and no Mn-oxide formed, are also in agreement with the XRD results in Fig. 2. This implied that MnO_x is amorphous and segregated at FePt grain boundaries, separating FePt grains. However, striking differences in morphology were observed when the FePt films were capped with the MnO_x of 41% O_2/Ar top layer during post-annealing. Fig. 4(b) shows the morphology of annealed 41% O_2/Ar FePt/MnO_x bilayer film. First, well-separated FePt grains (with the averaged grain size of 7 nm) by MnO_x are observed. Clearly, the role of the top MnO_x layer during post-annealing is to form grain boundaries and to separate the FePt grains. This is attributed to the insolubility of MnO_x in the FePt as well as the lower surface energy of MnO_x [10], [19].

The dependence of $H_{c\perp}$ and various % O_2/Ar in annealed FePt/MnO_x bilayer films were shown in Fig. 5, in order to correlate the evolution in microstructures and magnetism. In Fig. 5, the perpendicular coercivity decreases with increasing % O_2/Ar. The decreased $H_{c\perp} \sim 8$ kOe was found in annealed 8% O_2/Ar FePt/MnO_x bilayers. This reduction to a more moderate coercivity while retained an enhanced S [Fig. 3] is comparable to those reported in the literature [18], [20]. In addition to the $H_{c\perp}$, the hysteresis loops of post-annealed FePt/MnO_x (8%–41% O_2/Ar) bilayer films were shown as the inset in Fig. 5. Although $H_{c\perp}$ of the annealed FePt/MnO_x bilayer film is slightly reduced to about 8 kOe by addition of MnO 8% O_2/Ar, the remanence is still high enough for magnetic recording application. However, further increasing MnO% O_2/Ar rapidly dropped down the $H_{c\perp}$ and remanence. The downgrade of the $H_{c\perp}$ is attributed to the reduction of a hard fct FePt phase as MnO_x incorporated into FePt during post-annealing. This is consistent with the phase structural result described above.

In our previous works [13], [14], it is confirmed that typical interconnected domain patterns were observed in pure FePt film, due to continuous FePt grains are present in samples without the oxide addition. Here, the surface morphology and magnetic domain structures of annealed 8% and 41% O_2/Ar FePt/MnO_x

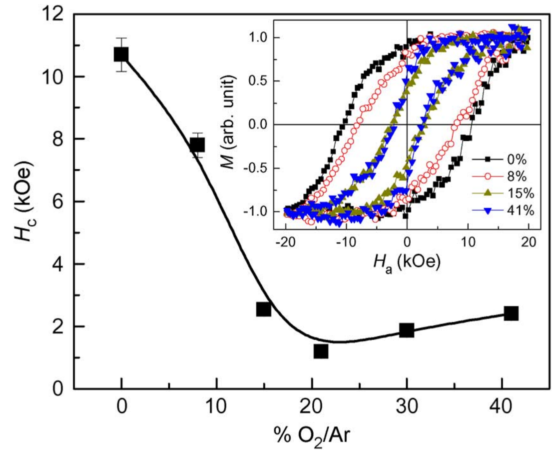

Fig. 5. Dependence of $H_{c\perp}$ and various % O_2/Ar in annealed FePt/MnO_x bilayer films. The inset shows the hysteresis loops of post-annealed FePt/MnO_x (8%–41% O_2/Ar) bilayer films. The annealing conditions are 550°C for 10 min.

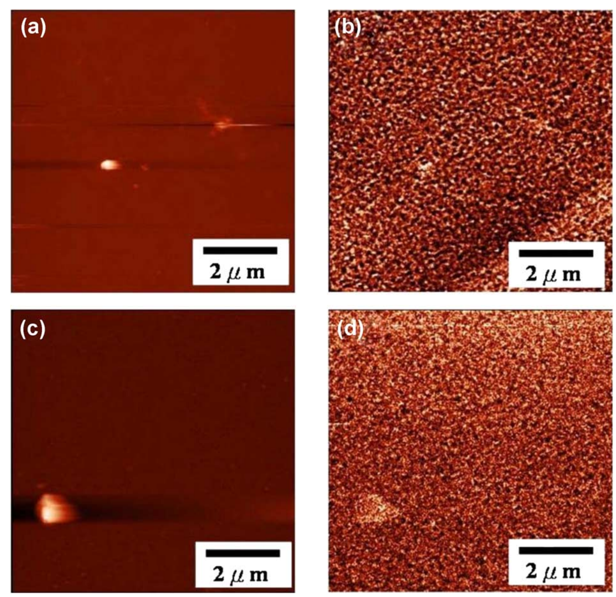

Fig. 6. AFM images of (a) the annealed FePt/MnO_x (8% O_2/Ar) bilayer, and (c) the annealed FePt/MnO_x (41% O_2/Ar) bilayer. The corresponding MFM images were shown in (b) and (d).

bilayer films were characterized by AFM and MFM for understanding the magnetic domain evolution as MnO_x incorporated into FePt. The results were shown in Fig. 6. The roughness of both samples are quite small $(R_a \sim 1\ \mathrm{nm})$ shown in Fig. 6(a) and (c), respectively. Therefore the signals in MFM images [Fig. 6(b) and (d)] are contributed from magnetic moment on FePt/MnO_x bilayer films. After comparing with Fig. 6(b) and (d), the clear magnetic contrast appeared in the 8% O_2/Ar FePt/MnO_x bilayer film, which is likely attributed to the strong stray field due to isolated magnetic FePt grains [11]. Further increased the oxide to 41% O_2/Ar, the decrease in contrast as well as the refined magnetic domain size were found, associating with the redistribution of FePt in MnO_x due to increasing amounts of MnO_x incorporated into the bottom FePt films during annealing. These results are in agreement with the microstructure observations and magnetic properties.

Combining the structural, microstructural, and magnetic properties, our results indicate strongly that the oxygen atoms present during the ion-beam bombardment process play an important role in determining the microstructure and magnetism of FePt/MnO_x bilayers during post-annealing. At lower % O_2/Ar, the oxygen atoms may occupy the interstitial positions in the FePt lattice. This in turn may induce a local strain thus enhancing the FePt ordering, S. However, at higher % O_2/Ar, the excess oxygen atoms act as diffusion barrier in the FePt grain growth by combing with Mn atoms to form grain boundary MnO_x. Any variations between order parameters (S) and coercivities (H_c) are likely due to inhomogeneities of FePt grains separated by grain boundary MnO_x. At lower MnO_x concentration (e.g., 8% O_2/Ar), isolated decoupled FePt grains (as revealed by TEM and MFM) experienced less barrier during magnetization reversal processes and thus a reduced coercivity was observed [Fig. 5]. However, further increased % O_2/Ar to over 21% O_2/Ar, the excess oxygen atoms may serve as defects to impede the magnetic reversal process and thus increase the coercivity [Fig. 5]. This gives rise to the increased H_c from 21% to 41% O_2/Ar in Fig. 5. We emphasize that an enhanced order parameter with moderate coercivity was achieved by the MnO_x capped layer through the annealing process. Further investigation to elucidate the distribution of MnO_x into the FePt layers by high resolution transmission electron microscopy (HRTEM) as well as Auger electron spectroscopy/electron spectroscopy for chemical analysis (AES/ESCA) is in progress.

IV. Conclusion

The microstructure and magnetic properties of FePt/MnO_x bilayers were investigated by ion bombardment deposition. The phase transformation from fcc FePt into $L1_0$ FePt gives rise to the enhanced coercivity during post-annealing. With increasing % O_2/Ar, the FePt grains are refined and well isolated by grain boundary MnO_x. The annealed FePt/MnO_x (8% O_2) bilayer exhibited the largest order parameter $S(\sim 0.85)$ while maintaining a moderate coercivity $(H_c \sim 8\,\mathrm{kOe})$. The enhanced S is likely created by the local strain due to the oxygen atoms (created by the ion-beam bombardment) occupying the interstitial positions in the FePt lattice. Our results indicate that the addition of MnO_x combining with annealing can effectively enhance the FePt ordering as well as the refinement of FePt grains.

Acknowledgment

This work was supported by the Ministry of Economic Affairs of Taiwan (98-EC-17-A-08-S1-006), National Science Council of Taiwan (NSC99-2218-E-155-006-MY2), and Seed Funding for Basic Research of the University of Hong Kong.

References

[1] J. Zhu and H. N. Bertram, "Reversal mechanisms and domain structures in thin-film recording media," *J. Appl. Phys.*, vol. 69, p. 9084-6089, April 1991.

[2] A. Cebollada, D. Weller, J. Sticht, R. Harp, R. F. C. Farrow, R. F. Marks, R. Savoy, and J. C. Scott, "Enhanced magneto-optical Kerr effect in spontaneously ordered FePt alloys: Quantitative agreement between theory and experiment," *Phys. Rev. B*, vol. 50, pp. 3419–3422, Aug. 1994.

[3] J.-I. Ikemoto and S. Nakagawa, "Fabrication of ultrathin FePt(Cu) ordered alloy thin films directly on glass disks from Pt(Cu)/Fe bilayers," *J. Appl. Phys.*, vol. 103, pp. 07B512-1–07B512-3, Feb. 2008.

[4] J.-U. Thiele, L. Folks, M. F. Toney, and D. K. Weller, "Perpendicular magnetic anisotropy and magnetic domain structure in sputtered epitaxial FePt (001) $L1_0$ films," *J. Appl. Phys.*, vol. 84, pp. 5686–5692, Nov. 1998.

[5] T. Suzuki, N. Honda, and K. Ouchi, "Magnetization reversal process in polycrystalline ordered Fe-Pt(001) thin films," *J. Appl. Phys.*, vol. 85, pp. 4301–4303, Apr. 1999.

[6] C. H. Lai, C. H. Yang, C. C. Chiang, T. Balaji, and T. K. Tseng, "Dynamic stress-induced low-temperature ordering of FePt," *Appl. Phys. Lett.*, vol. 85, pp. 4430–4432, Nov. 2004.

[7] Y. F. Ding, J. S. Chen, B. C. Lim, J. F. Hu, B. Liu, and G. Ju, "Granular $L1_0$ $\mathrm{FePt}:\mathrm{TiO_2}$ (001) nanocomposite thin films with 5 nm grains for high density magnetic recording," *Appl. Phys. Lett.*, vol. 93, pp. 032506-1–032506-3, July 2008.

[8] Z. L. Zhao, J. S. Chen, J. Ding, J. B. Yi, B. H. Liu, and J. P. Wang, "Fabrication and microstructure of high coercivity FePt thin films at 400 °C," *Appl. Phys. Lett.*, vol. 88, pp. 052503-1–052503-3, Feb. 2006.

[9] D. Weller, A. Moser, L. Folks, M. E. Eest, W. Lee, M. F. Toney, M. Schwickert, J.-U. Thiele, and M. F. Doerner, "High K_u materials approach to 100 $\mathrm{Gbits/in^2}$," *IEEE Trans. Magn.*, vol. 36, pp. 10–15, Jan. 2000.

[10] Y. C. Wu, L. W. Wang, and C. H. Lai, "Low-temperature ordering of (001) granular FePt films by inserting ultrathin SiO_2 layers," *Appl. Phys. Lett.*, vol. 91, pp. 072502-1–072502-3, Aug. 2007.

[11] A. C. Sun, J.-H. Hsu, P. C. Kuo, and H. L. Huang, "Microstructural and magnetic studies of $L1_0$ $\mathrm{FePt}-\mathrm{SiO_2}$ nano-composite thin film with columnar structure for perpendicular magnetic recording," *J. Magn. Magn. Mater.*, vol. 320, pp. 3071–3074, Aug. 2008.

[12] K. K. M. Pandey, J. S. Chen, G. M. Chow, and J. F. Hu, " $L1_0$ $\mathrm{CoPt}-\mathrm{Ta_2O_5}$ exchange coupled multilayer media for magnetic recording," *Appl. Phys. Lett.*, vol. 94, pp. 232502-1–232502-3, June 2009.

[13] K.-W. Lin, Y.-L. Chiu, A.-C. Sun, J.-H. Hsu, J. van Lierop, and T. Suzuki, "Ion-beam bombarded SiO_2 layer effects on the microstructure and magnetism in $\mathrm{FePt/SiO_2}$ bilayers," *Jpn. J. Appl. Phys.*, vol. 48, pp. 073002-1–073002-4, July 2009.

[14] J.-Y. Guo, C.-Y. Liu, H. Ouyang, K.-W. Lin, C.-J. Tsai, J. van Lierop, N. N. Phuoc, and T. Suzuki, "Effects of ion-beam bombardment and post-annealing on the structural and magnetic properties of Fe/Pt multilayers," *Phys. Stat. Sol. (c)*, vol. 4, pp. 4512–4515, Dec. 2007.

[15] K.-W. Lin, J.-Y. Guo, S.-R. Lin, H. Ouyang, C.-J. Tsai, J. van Lierop, N. N. Phuoc, and T. Suzuki, "Structural and magnetic properties of ion-beam bombarded Co/Pt multilayers," *Phys. Stat. Sol. (c)*, vol. 4, pp. 4507–4511, Dec. 2007.

[16] J. van Lierop, B. W. Southern, K.-W. Lin, Z.-Y. Guo, C. L. Harland, R. A. Rosenberg, and J. W. Freeland, "Exchange bias in a columnar nanocrystalline $\mathrm{Ni_{80}Fe_{20}/CoO}$ thin film," *Phys. Rev. B*, vol. 76, pp. 224432-1–224432-7, Dec. 2007.

[17] K.-W. Lin, J.-Y. Guo, H.-Y. Liu, H. Ouyanga, D.-H. Wei, and J. van Lierop, "Anomalous exchange bias behavior in ion-beam bombarded NiCo/(Ni, Co)O bilayers," *J. Appl. Phys.*, vol. 103, pp. 07C105-1–07C105-3, Jan. 2008.

[18] Y. K. Takahashi, T. Koyama, M. Ohnuma, T. Ohkubo, and K. Hono, "Size dependence of ordering in FePt nanoparticles," *J. Appl. Phys.*, vol. 95, pp. 2690–2696, March 2004.

[19] C. L. Platt, K. W. Wierman, J. K. Howard, A. G. Roy, and D. E. Laughlin, "A comparison of FePt thin films with HfO_2 or MnO additive," *J. Magn. Magn. Mater.*, vol. 260, pp. 487–491, Oct. 2003.

[20] B. Yao and K. R. Coffey, "The effective interdiffusivity, structure, and magnetic properties of $\mathrm{[Fe/Pt]_n}$ multilayer films," *J. Appl. Phys.*, vol. 103, pp. 07E107-1–07E107-3, Jan. 2008.